

November 2005

Image method solutions for free-particle wave packets in wedge geometries

R. W. Robinett*

Department of Physics

The Pennsylvania State University

University Park, PA 16802 USA

(Dated: July 9, 2021)

Abstract

Using analogs of familiar image methods in electrostatics and optics, we show how to construct closed form wave packet solutions of the two-dimensional free-particle Schrödinger equation in geometries restricted by two infinite wall barriers separated by an angle $\Theta_N = \pi/N$. As an example, we evaluate probability densities and expectation values for a zero-momentum wave packet solution initially localized in a $\Theta_3 = \pi/3 = 60^\circ$ wedge. We review the time-development of zero-momentum wave packets placed near a single infinite wall barrier in an Appendix.

PACS numbers: 03.65.-w, 03.65.Ca, 03.65.Ge, 03.65.Sq

*Electronic address: rick@phys.psu.edu

I. INTRODUCTION

Examples of closed-form wave packet solutions of the time-dependent Schrödinger equation (SE) in introductory quantum mechanics are at a premium. A few standard books treat the case of wave packets for the harmonic oscillator (either coherent or squeezed state versions), often using methods which are rather advanced, such as propagator techniques [1]. Almost all standard texts, however, develop the explicit example of the free-particle Gaussian wave packet, which requires only simple integration, and which yields a closed form solution. These solutions can, in turn, be used to easily evaluate many expectation values and examine both semi-classical propagation as well as wave packet spreading.

A simple generalization of that example to a slightly more ‘interacting’ case is that of the single infinite wall in one-dimension (or particle on the half-line) defined by the potential

$$V(x) = \begin{cases} 0 & x > 0 \\ \infty & x \leq 0 \end{cases} . \quad (1)$$

Andrews [2] has noted that simple linear combination solutions of the form

$$\tilde{\psi}(x, t) = \begin{cases} \psi(x, t) - \psi(-x, t) & x \geq 0 \\ 0 & x \leq 0 \end{cases} \quad (2)$$

will also satisfy the Schrödinger equation for $x > 0$, provided that $\psi(x, t)$ is a 1D free-particle solution, since the free-particle Hamiltonian is invariant under $x \longleftrightarrow -x$. This form is then seen to also satisfy the necessary boundary condition at the infinite wall barrier for all times. Such mirror solutions have been used to pedagogically examine the detailed nature of the ‘collision’ of a wave packet with such an infinite wall barrier [3], for which many exact results are possible [4], as well as motivating discussions of possible experimental tests of the problem of the “*Deflection of quantum particles by impenetrable boundary*” [5].

A simple generalization of this ‘mirror’ problem to two-dimensions involves two infinite wall barriers placed at right angles (90°), defined by a potential

$$V_{90} = \begin{cases} 0 & \text{for } x > 0 \text{ and } y > 0 \\ \infty & \text{otherwise} \end{cases} \quad (3)$$

where the particle is constrained to be in the first (upper-right) quadrant. Product solutions,

using ‘mirror’ combinations as above, of the form

$$\tilde{\psi}(x, y; t) = \begin{cases} [\psi_1(x, t) - \psi_1(-x, t)][\psi_2(y, t) - \psi_2(-y, t)] & \text{for } x \geq 0 \text{ and } y \geq 0 \\ 0 & \text{otherwise} \end{cases} \quad (4)$$

satisfy the 2D Schrödinger equation for $x, y > 0$, as well as the boundary conditions on the two intersecting infinite barriers. The form of the product wavefunction in the first quadrant,

$$\begin{aligned} \tilde{\psi}_1(x, t)\tilde{\psi}_2(y, t) = & \psi_1(x, t)\psi_2(y, t) - \psi_1(x, t)\psi_2(-y, t) - \psi_1(-x, t)\psi_2(y, t) \\ & + \psi_1(-x, t)\psi_2(-y, t) \end{aligned} \quad (5)$$

suggests that an even more general form, namely

$$\tilde{\psi}(x, y; t) = \xi(x, y; t) - \xi(x, -y; t) - \xi(-x, y; t) + \xi(-x, -y; t), \quad (6)$$

will satisfy the appropriate SE (for any $\xi(x, y; t)$ which does) since the 2D free-particle Hamiltonian is invariant under both $x \longleftrightarrow -x$ and $y \longleftrightarrow -y$. The additional terms in Eqn. (6) correspond to two ‘mirror’ terms reflected in each infinite wall barrier (flipped in sign) with an additional term (with the original sign) arising from two reflections, all terms being necessary in order to satisfy the boundary conditions on both infinite wall barriers.

Thought of in this way, such solutions are immediately reminiscent of image solutions to the related problem of two perpendicular conducting plates in electrostatics or the even more fundamental problem of the images of a single real object as seen in a pair of mirrors placed at right angles. The pattern of ‘signs’ used in each of those two cases is identical to that seen in Eqn. (6). This suggests that a much wider variety of ‘two-wall’ problems in quantum mechanics can be constructed using ones intuition from such classical textbook examples.

The potential in Eqn. (3) is a specific case of two infinite barriers intersecting with an arbitrary angle Θ , defined by

$$V_{\Theta}(r, \theta) = \begin{cases} 0 & \text{if } r > 0 \text{ and } 0 < \theta < \Theta \\ \infty & \text{otherwise} \end{cases} . \quad (7)$$

The corresponding electrostatic (or optics) problems for the special cases of $\Theta_N = \pi/N$ can be solved by making use of a finite number of virtual ‘image’ charges (or true images)

given by the following prescription. Place the original charge (or object) at a general point (x, y) within the allowed wedge region. Add a ‘mirror’ image charge (or object) at $(x, -y)$, but with opposite sign (handedness). Then repeatedly ($N - 1$ times) rotate the location of these two charges (or objects) through $\theta = 2\Theta_N$, keeping track of the appropriate sign (or handedness). For $\Theta = \Theta_N = \pi/N$, this process closes on itself, and the resulting set of $2N$ charges (or objects), $2N - 1$ of which are auxiliary ones, satisfies the boundary conditions for the problem. (The cases of $N = 1, 2$ correspond to the single infinite wall and the 90° wedge in Eqn. (3) respectively.) In the context of the 2D Schrödinger equation, such rotations of coordinates can be easily proved to leave the free-particle Hamiltonian invariant, so that a wavefunction of the form $\psi(x \cos(\phi) + y \sin(\phi), -x \sin(\phi) + y \cos(\phi); t)$ will be a solution if $\psi(x, y; t)$ is. This fact justifies the use of additional rotated versions of an existing free-particle solution in a linear combination, generalizing the result Eqn. (6) for the case of $N = 2$.

As an example of this construction and its relevance to the problem of two infinite wall barriers, consider the case of $\Theta_3 = 60^\circ$, as shown in Fig. 1, where the prescription above yields the five ‘image’ points shown there. Using the appropriate locations, and signs, it is possible to construct a general solution as

$$\begin{aligned} \psi_{60}(x, y; t) = & \psi(x, y; t) - \psi(x, -y; t) \\ & + \psi\left(-\frac{x}{2} - \frac{\sqrt{3}y}{2}, \frac{\sqrt{3}x}{2} - \frac{y}{2}; t\right) - \psi\left(-\frac{x}{2} + \frac{\sqrt{3}y}{2}, \frac{\sqrt{3}x}{2} + \frac{y}{2}; t\right) \\ & + \psi\left(-\frac{x}{2} + \frac{\sqrt{3}y}{2}, -\frac{\sqrt{3}x}{2} - \frac{y}{2}; t\right) - \psi\left(-\frac{x}{2} - \frac{\sqrt{3}y}{2}, -\frac{\sqrt{3}x}{2} + \frac{y}{2}; t\right). \end{aligned} \quad (8)$$

This can readily be seen to satisfy the boundary conditions on the two infinite walls, namely

$$\psi_{60}(x, y = 0; t) = 0 = \psi_{60}(x, y = \sqrt{3}x; t) \quad \forall x, t. \quad (9)$$

The results for the case of $\Theta = \pi/4 = 45^\circ$ and others are obtained in exactly the same way. We note that the 1D infinite square well has been discussed in terms of image methods [6], [7], requiring an infinite number of virtual terms, analogous to the optical case of two parallel mirrors. The $N \rightarrow \infty$ limit of small angle wedges ($\Theta_N \rightarrow 0$) is qualitatively different as it does not lead to bound states.

The standard 1D Gaussian free-particle solution with arbitrary initial central position

and momentum (x_0 and p_0) is given by

$$\psi_{(G)}(x, t) = \frac{1}{\sqrt{\sqrt{\pi}\beta(1 + it/t_0)}} e^{ip_0(x-x_0)/\hbar} e^{-ip_0^2 t/2m\hbar} e^{-(x-x_0-p_0 t/m)^2/2\beta^2(1+it/t_0)} \quad (10)$$

where

$$t_0 \equiv \frac{m\beta^2}{\hbar}, \quad \Delta x_0 = \frac{\beta}{\sqrt{2}}, \quad \text{and} \quad \Delta p_0 = \frac{\hbar}{\beta\sqrt{2}} \quad (11)$$

are the spreading time and initial spreads in position and momentum (for the free 1D particle) respectively.

Products of these of the form $\psi_{(G)}(x, t)\psi_{(G)}(y, t)$ can then be used in Eqn. (8) for any desired initial conditions. A simple example of a spreading wavepacket, corresponding to $(p_{y0}, p_{x0}) = (0, 0)$, initially near the corner of a $\Theta_3 = 60^\circ$ wedge, is shown in Fig. 2, illustrating the complex time-development possible.

For the case of the single infinite wall, and the $\Theta = \pi/2 = 90^\circ$ wedge, such an approach can be continued to include the exact normalization of the wave function if Gaussian components are used as well as in the evaluation of a number of expectation values and related quantities exactly [4]. For the cases of $\Theta = \pi/N$ with $N > 2$, the normalization integrals involve Airy functions and so cannot be done in as compact a closed form, but experience with simpler cases guarantees that if the individual ‘component’ terms (the original and image contributions) are sufficiently separated in phase space, i.e. if their central values of x_0, p_0 are far apart in units of the fundamental position/momentum spreads, Δx_0 and Δp_0 , then the normalization factors differ from unity by exponentially small terms.

These systems can be profitably discussed in introductory quantum mechanics courses, as non-trivial examples of the imposition of boundary conditions in a novel 2D geometry, in a free-particle context as opposed to more familiar bound state systems. In this context, the $\Theta = \pi/2$, $\pi/3$ and $\Theta = \pi/4$ cases can be compared to bound state quantum wells with related geometries, as special cases of wave propagation near a ‘corner’. The $N = 2$ case of two walls at right angles provides an example of relevance to the 2D square well, where the very short-term evolution of wave packets in that bound-state system would be that of just such a ‘corner reflector’, but with a more complex long-term time-dependence, including the possibility of quantum revivals. The $45^\circ - 45^\circ - 90^\circ$ triangular well (or quantum billiard) is soluble using the odd linear combination of degenerate eigenstates of the corresponding 2D square well, namely $\psi(x, y) = (u_n(x)u_m(y) - u_m(x)u_n(y))/\sqrt{2}$ (where $m \neq n$) which satisfies the boundary conditions on the sides of the square, but also along the $y = x$

diagonal boundary. The case of an equilateral ($60^\circ - 60^\circ - 60^\circ$) triangle infinite well is also known (perhaps not nearly as well as it should be) to also have simple closed form energy-eigenstate solutions [8] and the $\Theta_3 = 60^\circ$ wedge can be thought of as one ‘corner’ of that triangular billiard. (The construction of wave packets in all three bound state systems has been discussed in a pedagogical context in Ref. [9].)

The ability to manipulate relatively simple closed-form solutions enables a wide variety of visualizations to be easily generated, so students can examine the analogs of many classical ‘bouncing’ trajectories, including more complex ones than the simple ‘in-and-out’ paths for the $N = 2$ ‘corner reflector’. More sophisticated projects involving the numerical evaluation of time-dependent expectation values (to be compared with classical expectations) or of the momentum-space probability densities are now more within reach since a closed-form solution for $\psi(x, y; t)$ already exists. For example, while a classical particle placed near the corner of a wedge would remain at rest, Fig. 2 suggests that the long-term expectation values of $\langle x \rangle_t$ and $\langle p \rangle_t$ will have interesting non-classical behavior. To examine just this effect, the time-dependent expectation values $\langle x \rangle_t$ and $\langle y \rangle_t$ for that case are evaluated numerically and shown in Fig. 3 for the same parameter set as in Fig. 2. We note in this case that the long-term values of $\langle p_x \rangle_t$ and $\langle p_y \rangle_t$, evaluated using the basic relation $\langle p_x \rangle_t = md\langle x \rangle_t/dt$, can be seen to satisfy $\tan(\theta) = \langle p_y \rangle_t / \langle p_x \rangle_t \approx 0.577$ giving $\theta = 30^\circ$ to a very high numerical accuracy; thus, the wave packet develops in time in a manner consistent with its restricted geometry. The interplay between the generation of non-zero values of the expectation values of momenta and the conservation of kinetic energy are questions which arise naturally to students when examining such systems. These are perhaps more easily addressed in the context of a single infinite wall (the $N = 1$ case, as discussed in Ref. [5]) and we review some aspects of those questions in Appendix A.

Finally, and perhaps more importantly, the notion of multiple Gaussian wavepackets overlapping and demonstrating interference phenomena, such as seen in Fig. 2, is a useful introduction or way to motivate the study of famous experiments which have shown the “*Observation of interference between two Bose condensates*” (as first discussed in Ref. [10], but also observed in Ref. [11], and subsequently extended to see matter wave interference between large numbers of BEC’s [12].) Such experiments have been analyzed [13] in terms of linear combinations of localized Gaussian wave packets, allowed to expand after being released, and exhibiting the observed interference behavior as they overlap. One can imag-

ine [14] single BEC's released near one or more infinite wall boundaries (modeling atomic mirrors) being described by a wave function solution much like that in Eqns. (2), (6), or (8), discussed here in a more pedagogical context.

APPENDIX A: MOMENTUM AND KINETIC ENERGY FOR A ZERO-MOMENTUM 1D WAVE PACKET IMPINGING ON AN INFINITE WALL

For a classical point particle rebounding elastically from a wall, the impulsive change in momentum (from $\pm p_0$ to $\mp p_0$) and the fact that the total kinetic energy is unchanged (since $T = p^2/2m$), have analogs in the interactions of a quantum wave packet with a 1D infinite wall [3], [4]. The time-development of the expectation values of momentum, kinetic energy, and the spread in momentum for a initially 'zero-momentum' wave packet expanding near an infinite wall can easily raise related questions which can be nicely visualized, understood intuitively, and for which long-time approximations can be derived, all aspects which we review in this Appendix.

In Fig. 4, we plot the position-space ($|\tilde{\psi}(x, t)|^2$ versus x) and momentum-space ($|\tilde{\phi}(p, t)|^2$ versus p) distributions for a simple 'mirror' solution of the form in Eqn. (2) using a Gaussian $\psi_{(G)}(x, t)$ with $p_0 = 0$. The momentum-space wave function is obtained by numerical Fourier transform of the closed-form $\tilde{\psi}(x, t)$. A free-particle $p_0 = 0$ Gaussian wave packet would simply spread, while maintaining its Gaussian form, with an increasing uncertainty in position given by $\Delta x_t = \Delta x_0 \sqrt{1 + (t/t_0)^2}$; the corresponding momentum-space probability distribution, $|\phi(p, t)|^2$, would remain unchanged, since $\phi(p, t) = \phi(p, 0) \exp(-ip^2 t/2m\hbar)$ for the 1D free-particle.

For this case of the 1D infinite barrier, however, the wave packet components which move towards the wall ($p < 0$) must rebound, flipping sign and combine with the right-moving ($p > 0$) values which are not flipped, yielding an overall non-zero value of the expectation value of momentum, as shown by the vertical dotted lines in the $|\tilde{\phi}(p, t)|^2$ plots on the right of Fig. 4. The negative values of momentum in the initial $\tilde{\phi}(p, 0)$ are, roughly speaking, 'folded over' on top of the positive values after reflection in sign, yielding a distribution which is therefore also narrower; a crude estimate based on this picture would be that the momentum-space spread would be roughly half as large as its initial value. For increasingly large time, any small negative components will eventually rebound from the wall so that

$|\tilde{\phi}(p, t)|^2$ becomes non-vanishing only for $p > 0$.

For any free-particle solution, the expectation value of the kinetic energy, given by $\langle T \rangle = \langle p^2 \rangle / 2m$, will remain fixed, but the relation

$$\frac{\hbar^2}{2\beta^2} \approx \langle p^2 \rangle_0 = \langle p^2 \rangle_t = \langle p \rangle_t^2 + (\Delta p_t)^2 \quad (\text{A1})$$

allows for a non-zero value of $\langle p \rangle_t$ to develop (as it does here, for the physical reasons mentioned above) but at the expense of a smaller width in momentum-space (because the negative components are ‘flipped’ on top of the corresponding positive ones.)

The interference structure seen in the momentum-space probability density can also be understood from simple arguments. Momentum components labeled by p will have an associated wavelength of $\lambda = 2\pi\hbar/p$ and as the wave packet spreads (and interferes with its ‘mirror image’) there can be destructive interference between $\psi(x, t)$ and $\psi(-x, t)$ (destructive because of the sign difference in Eqn. (2)) when $n\lambda = 2x_0$ or when $p = n(\pi\hbar/x_0)$. (This type of interference structure in the momentum-space probability density has been studied in the context of Bose-Einstein condensates [15] and is a general feature of the overlap of two (or more) expanding Gaussians.)

An excellent approximation to the long-term ($t \gg t_0$) form of $\tilde{\phi}(p, t)$ can be derived by first considering the linear combination of free-particle Gaussian momentum-space solutions, namely

$$\begin{aligned} \phi(p, t) &= \frac{N}{\sqrt{2}} \left(\sqrt{\frac{\alpha}{\sqrt{\pi}}} e^{-\alpha^2 p^2 / 2} e^{-ip^2 t / 2m\hbar} e^{-ipx_0 / \hbar} - \sqrt{\frac{\alpha}{\sqrt{\pi}}} e^{-\alpha^2 p^2 / 2} e^{-ip^2 t / 2m\hbar} e^{+ipx_0 / \hbar} \right) \\ &= -2Ni \sqrt{\frac{\alpha}{\sqrt{2\pi}}} \sin\left(\frac{px_0}{\hbar}\right) e^{-\alpha^2 p^2 / 2} e^{-ip^2 t / 2m\hbar}. \end{aligned} \quad (\text{A2})$$

The two contributions differ only in their central location, determined by the $\exp(\pm ipx_0 / \hbar)$ terms, corresponding to the $\psi(x, t)$ and $\psi(-x, t)$ terms. The normalization factor, N , is exponentially close to unity if $2x_0 \gg \beta$ and $\alpha \equiv \beta / \hbar$. For the ‘mirror’ solution in Eqn. (2), the Fourier transform of $\tilde{\psi}(x, t)$ required to obtain $\tilde{\phi}(p, t)$ initially only samples the isolated Gaussian term peaked at $+x_0$, giving the standard Gaussian form for both $\tilde{\psi}(x, 0)$ and $\tilde{\phi}(p, 0)$ as shown in Fig. 4. For very long times, however, when both terms in the ‘mirror solution’ have had time to expand and overlap substantially, the Fourier integration over $x \geq 0$ increasingly samples contributions from both $\psi(x, t)$ and $\psi(-x, t)$ more evenly, giving a result for the associated $\tilde{\phi}(p, t)$ which is close to that in Eqn. (A2), but with an additional

factor of $\sqrt{2}$ (to ensure proper normalization) since it's eventually restricted to $p > 0$. This gives an approximate expression for the momentum-space probability density of

$$|\tilde{\phi}(p, t \gg t_0)|^2 \approx \frac{4\alpha}{\sqrt{\pi}} \sin\left(\frac{px_0}{\hbar}\right)^2 e^{-\alpha^2 p^2} \quad (\text{A3})$$

for $p > 0$ and zero otherwise, and this form exhibits zeros at integral multiples of $p = \pi\hbar/x_0$. This limiting case is also plotted in Fig. 4 (as the dashed curves on the right) and the numerically obtained results do approach that form for long times. The long-term value of the expectation value of momentum can also be approximated by noting that

$$\langle p \rangle_{t \gg t_0} \approx \int_0^{+\infty} p \left[\frac{4\alpha}{\sqrt{\pi}} \sin\left(\frac{px_0}{\hbar}\right)^2 e^{-\alpha^2 p^2} \right] dp \approx \frac{1}{\alpha\sqrt{\pi}} \quad (\text{A4})$$

where we approximate the oscillating $\sin^2(px_0/\hbar)$ term by its average of 1/2. This then gives

$$\Delta p_{t \gg t_0} \approx \sqrt{\frac{(\pi - 2)}{2\pi\alpha^2}} = \left[\sqrt{\frac{\pi - 2}{\pi}} \right] \left(\frac{\hbar}{\sqrt{2}\beta} \right) \approx 0.6\Delta p_0 \quad (\text{A5})$$

which is what is observed numerically for $t \gg t_0$ and which is close to the crude estimate mentioned above. (Note that a similar expression was found in Ref. [3] for the spread in position of a Gaussian wave packet as it hits an infinite wall and is temporarily compressed.)

-
- [1] Saxon D S 1968 *Elementary Quantum Mechanics* (San Francisco: Holden-Day) pp 144-147
 - [2] Andrews M 1998 *Wave packets bouncing off walls* Am. J. Phys. **66** 252-254
 - [3] Doncheski M A and Robinett R W 1999 *Anatomy of a quantum 'bounce'* Eur. J. Phys. **20** 29-37
 - [4] Belloni M, Doncheski M A, and Robinett R W 2005 *Exact results for 'bouncing' Gaussian wave packets* Phys. Scripta **71** 136-140
 - [5] Dodonov V V and Andreatta, M A 2000 *Deflection of quantum particles by impenetrable boundary* Phys. Lett. **A275** 173-181; 2002 *Quantum deflection of ultracold atoms from mirrors* Laser Phys. **12** 57-70; Andreatta M A and Dodonov V V 2002 *The reflection of narrow slow quantum packets from mirrors* J. Phys. A: Math. Gen. **35** 8373-8392
 - [6] Kleber M 1994 *Exact solutions for time-dependent phenomena in quantum mechanics* Phys. Rep. **236**, 331-393.

- [7] Born M 1955 *Continuity, determinism, and reality*, Kgl. Danske Videns. Sels. Mat.-fys. Medd., **30** (2) 1; Born was addressing concerns made by A. Einstein 1953 *Elementare Überlegungen zur Interpretation der Grundlagen der Quanten-Mechanik*, in *Scientific papers presented to Max Born* (Edinburgh: Oliver and Boyd) pp 33-40; Born M and Ludwig W 1958 *Zur Quantenmechanik der kräftefreien Teilchens*, Z. Phys. **150** 106-117
- [8] Mathews J and Walker R L 1970 *Mathematical Methods of Physics*, 2nd edition (Menlo Park: W. A. Benjamin) pp. 237-239; Jung C 1980 *An exactly soluble three-body problem in one-dimension* Can. J. Phys. **58** 719-728; Richens P J and Berry, M V 1981 *Pseudointegrable systems in classical and quantum mechanics*, Physica **2D** 495-512; Li W -K and Blinder S M 1987 *Particle in an equilateral triangle: Exact solution of a nonseparable problem*, J. Chem. Educ. **64** 130-132; Doncheski M A and Robinett R W 2002 *Quantum mechanical analysis of the equilateral triangle billiard: periodic orbit theory and wave packet revivals*, Ann. Phys. (New York) **299** 208-227 [arXiv:quant-ph/0307063]
- [9] Doncheski M A, Heppelmann S, Robinett R W, and Tussey D C 2003 *Wave packet construction in two-dimensional quantum billiards: Blueprints for the square, equilateral triangle and circular cases* Am. J. Phys. **71**, 541-557 [arXiv:quant-ph/0307070]
- [10] Andrews M R, Townsend C G, Miesner H -J, Durfee D S, Kurn D M, and Ketterle W 1997 *Observation of interference between two Bose condensates* Science **275** 637-641; Durfee D S and Ketterle W 1998 *Experimental studies of Bose-Einstein condensates* Optics Express **2** 299-313
- [11] Hagley E W, Deng L, Kozuma M, Trippenbach M, Band Y B, Edwards M, Doery M, Julienne P S, Helmeson K, Rolston S L and Phillips W D *Measurement of the coherence of a Bose-Einstein condensate* 1999 Phys. Rev. Lett. **83** 3112-3115
- [12] Hadzibabic Z, Stock S, Battelier B, Bretin, V, and Dalibard J *Interference of an array of Bose-Einstein condensates* 2004 Phys. Rev. Lett. **93** 180403
- [13] Wallis H, Röhrl A, Naraschewski M, and Schenzle A 1997 *Phase-space dynamics of Bose condensates: Interference versus interaction* Phys. Rev. **A55** 2109-2119
- [14] Robinett R W 2005 *Self-interference of a single Bose-Einstein condensate due to boundary effects* to appear in Physica Scripta [arXiv:quant-ph/0511075]
- [15] Pitaevskii L and Strigari S 1999 *Interference of Bose-Einstein condensates in momentum space* Phys. Rev. Lett. **83** 4237-4240

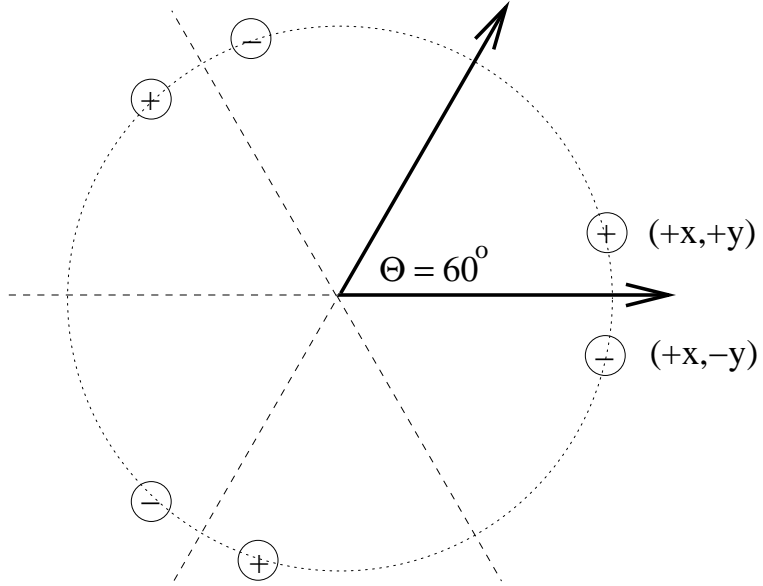


FIG. 1: Image construction for the $\Theta_3 = \pi/3 = 60^\circ$ wedge potential, leading to the solution in Eqn. (8).

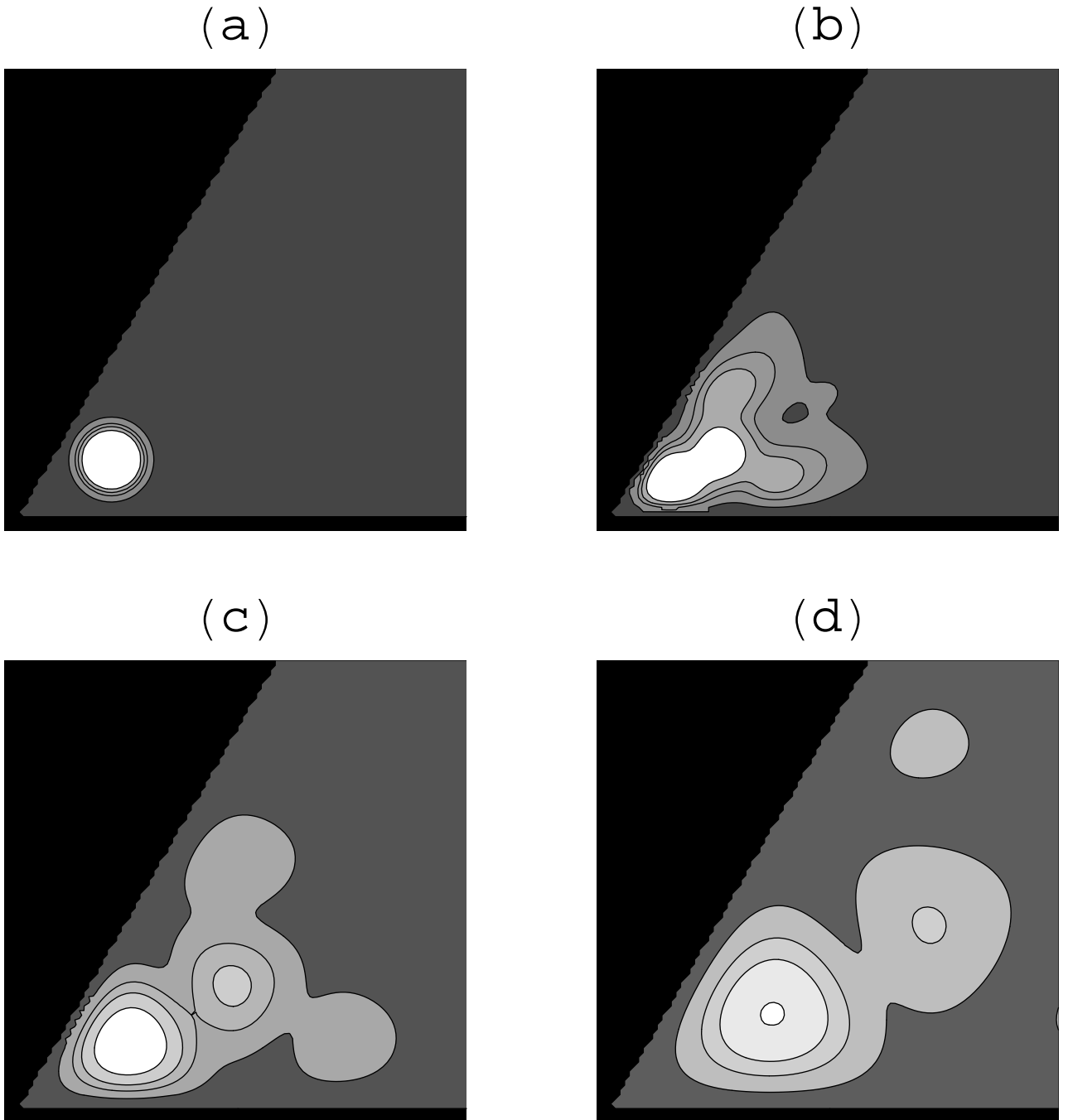


FIG. 2: Contour plot of the probability density ($|\psi(x, y; t)|^2$ versus (x, y)) for a spreading wave packet in the $\Theta_3 = 60^\circ$ wedge, using the solution in Eqn. (8) with individual terms being a product of Gaussian forms as in Eqn. (10). The example shown here has $(p_{x0}, p_{y0}) = (0, 0)$ and $(x_0, y_0) = (5, 3)$. Numerical values of $\hbar, m, \beta = 1$ are used which give $t_0 = 1$ as well. The (a)-(d) cases shown correspond to $t = 0, 5, 10, 15$ in these units.

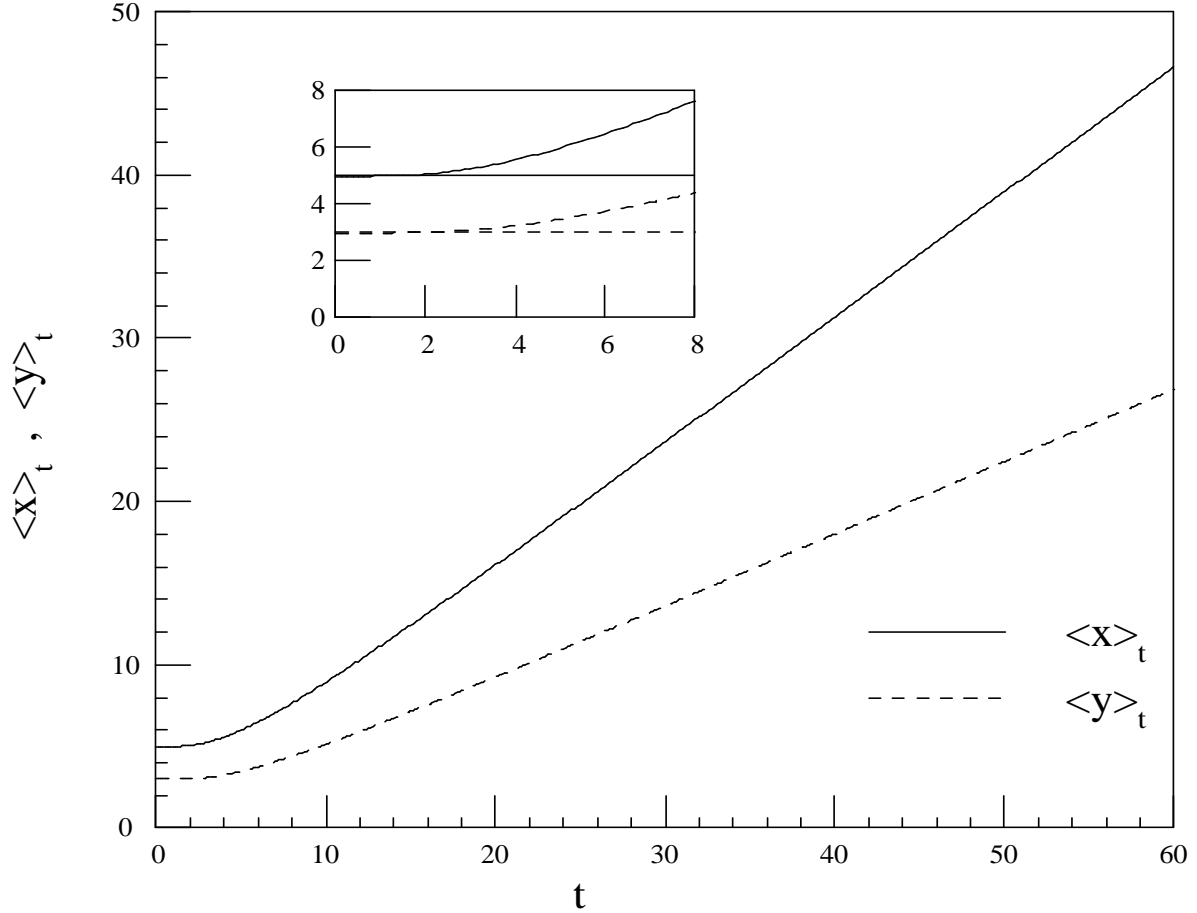


FIG. 3: Expectation values, $\langle x \rangle_t$ and $\langle y \rangle_t$ versus t , for the zero-momentum initial state shown in Fig. 2. The insert shows the short-term time-development, initially consistent with the (stationary) expansion of a zero-momentum wave packet, until the higher momentum components begin to reflect from the infinite wall boundaries, giving non-zero values of $\langle p_x \rangle_t$ and $\langle p_y \rangle_t$.

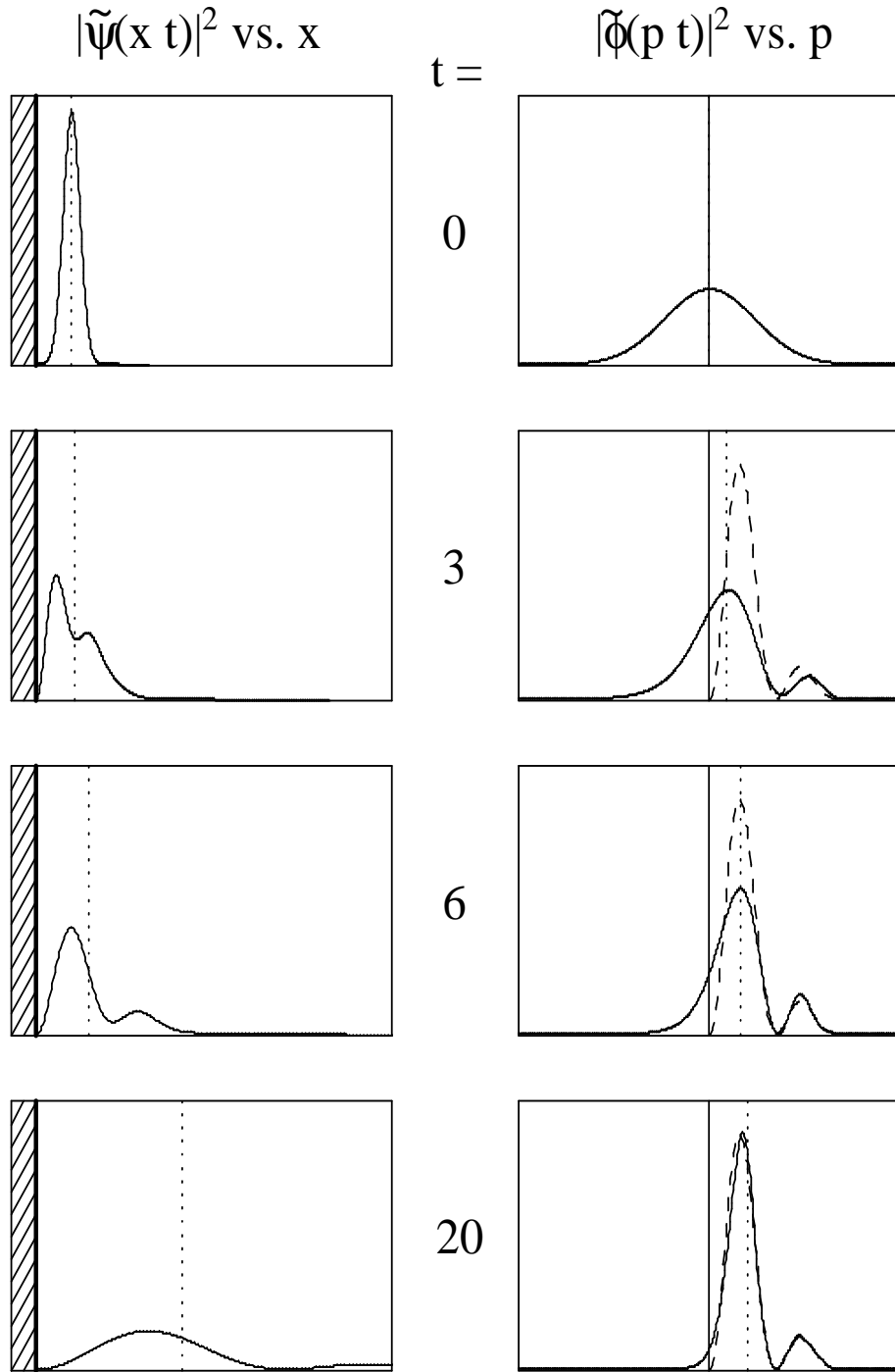


FIG. 4: Plots of the position-space (left) and momentum-space (right) probability densities versus time for a $p_{0x} = 0$ wavepacket allowed to expand near an infinite wall. The vertical dotted lines show the time-dependent expectation values $\langle x \rangle_t$ (left) and $\langle p \rangle_t$ (right). The dashed curve on the right is the $t \gg t_0$ solution from Eqn. (A3). Values of $x_0 = 3$ and $\hbar, \beta, m = 1$ are used, giving $t_0 = 1$.